Robustness properties of hill-climbing algorithm based on Zernike modes for laser beam correction

Ying Liu,[1] Jianqiang Ma,[1,2] Junjie Chen,[1] Baoqing Li,[1,*] and Jiaru Chu[1]

[1]Department of Precision Machinery and Precision Instrumentation, University of Science and Technology of China, Hefei, Anhui 230027, China

[2]Faculty of Mechanical Engineering & Mechanics, Ningbo University, Fenghua Road 818, Ningbo 315211, China

*Corresponding author: bqli@ustc.edu.cn

Received 30 October 2013; revised 23 January 2014; accepted 27 January 2014; posted 28 January 2014 (Doc. ID 200445); published 28 February 2014

A modified hill-climbing algorithm based on Zernike modes is used for laser beam correction. The algorithm adopts the Zernike mode coefficients, instead of the deformable mirror actuators' voltages in a traditional hill-climbing algorithm, as the adjustable variables to optimize the object function. The effect of the mismatches between the laser beam and the deformable mirror both in the aperture size and the center position was analyzed numerically and experimentally to test the robustness of the algorithm. Both simulation and experimental results show that the mismatches have almost no influence on the laser beam correction, unless the laser beam exceeds the effective aperture of the deformable mirror, which indicates the good robustness of the algorithm. © 2014 Optical Society of America

OCIS codes: (220.1010) Aberrations (global); (110.1080) Active or adaptive optics; (140.3300) Laser beam shaping.

http://dx.doi.org/10.1364/AO.53.00B140

1. Introduction

Adaptive optics (AO) is a well-established technique for correcting wavefront aberrations of the laser beam and improving beam quality, which thereby can improve the performance for fabrication or imaging of the system. The AO technique has been developed quickly and plays important roles in astronomical imaging [1,2], vision science [3,4], microscopy [5,6], and high-energy lasers [7,8].

The wavefront sensor-less AO system has been widely used for laser beam correction applications, since this system has a relatively simple structure compared to the traditional AO system with a wavefront sensor. In the wavefront sensor-less AO system, the optimization algorithm is adopted to find an appropriate set of control voltages from the sets that form the solution space. Various kinds of model-free stochastic algorithms, such as hill-climbing algorithm (HC) [9], genetic algorithm (GA) [10,11], stochastic parallel gradient descent (SPGD) [12,13], and simulated annealing algorithm (SA) [14,15], have been used for laser beam correction. Alternatively, several algorithms based on Zernike modes have also been proposed for their fast-converging speed. For example, the algorithm based on Zernike mode has been used in laser beam aberration correction to improve the confocal microscope imaging resolution [6], and the GA based on Zernike mode has been used in intracavity transverse modes control for the Nd:YAG solid laser [16].

A modified hill-climbing algorithm based on Zernike modes (ZMHC) adopts the Zernike mode coefficients as the adjustable variables to optimize the object function [17], while a traditional HC algorithm uses the DM actuators voltages. This ZMHC algorithm has been proved to have an ability to correct the aberrations of the laser beam with a fast speed. However, in practical application for laser beam

1559-128X/14/10B140-07$15.00/0

correction, the diameter of the laser beam may not be exactly equal to the effective aperture of the deformable mirror, and the center of the laser beam is possibly misaligned to that of the deformable mirror. The effect of these mismatches on correction results based on such the aforementioned modal algorithm has not been researched yet. In this paper, the effect of the mismatches for laser beam correction will be investigated by simulation and experiment.

2. Principle of ZMHC Algorithm

It is known that for small aberration the Strehl ratio (SR) of a laser beam does not depend on the form of the wavefront aberrations but only on its variance [18]. And the SR can be expressed simply as

$$\mathrm{SR} \approx 1 - \sigma_\phi^2, \tag{1}$$

where $\phi(r,\theta)$ is the wavefront aberration and σ_ϕ^2 is the variance of the wavefront aberration. The r and θ are polar radius and angle in the aberration plane. As it is known, the aberrations $\phi(r,\theta)$ can be expressed as a series of N Zernike polynomials, which is denoted by $Z_n(r,\theta)$

$$\Phi(r,\theta) = \sum_{n=1}^{N} c_n Z_n(r,\theta). \tag{2}$$

As the finite modes Zernike polynomials of N are used, a residual aberration exists due to the truncation of Zernike polynomials. Here, this residual aberration is omitted, since it is usually very small. For the orthogonality of the Zernike modes, the variance of the aberration can be as

$$\sigma_\phi^2 = \sum_{n=1}^{N} c_n^2. \tag{3}$$

So the far field intensity I on the focal plane can be as

$$I \approx I_0\left(1 - \sum_{n=1}^{N} c_n^2\right), \tag{4}$$

where I_0 is the ideal intensity without aberrations.

In order to obtain the global maximum value of F, c_n should be adjusted to be 0 for n from 1 to N. Based on this principle, the ZMHC algorithm adopts the Zernike mode coefficients as the adjustable variables, replacing the actuator voltages in the traditional HC algorithm [17]. The procedure of the ZMHC algorithm is as follows: First, to adjust c_n to be 0, an increment Δc_n is added to c_n to judge the right adjusting direction, and second, c_n is adjusted in the right direction with the increment Δc_n continuously until the evaluation function becomes worse. In actual operations, the voltage increment Δv_n that generates the amount of the nth Zernike mode (equal to Δc_n) is applied to the control voltages to get the corresponding adjustment of c_n.

3. Mismatch Problems in Laser Beam Correction

In the ZMHC algorithm, the Zernike expansion and the increment Δc_n of the Zernike coefficient is calculated in a given circular field of the deformable mirror's effective aperture. However, the aperture diameters of the DM and the laser beam are difficult to match exactly. The size of the laser beam is usually decided by the specific applications. Since the deformable mirror is not specially designed for the application, the aperture diameter of the DM and the laser beam is difficult to match exactly. Though a telescope system can be used in some AO systems to match the apertures of the DM and the laser beam, the mismatch may still exist. In addition, it's also difficult to precisely align the center of the laser beam with the center of the DM's effective aperture. Therefore, the effect of the mismatches on correction results is analyzed in this study. The mismatch situations were categorized into three cases: Case I [Fig. 1(a)], the aperture of the laser beam does not match the effective aperture of the DM. Case II [Fig. 1(b)], the center of the laser beam is not aligned to that of the effective aperture of the DM but does not exceed the DM's effective aperture. Case III [Fig. 1(c)], the two centers are not aligned, and the laser beam exceeds the DM's effective aperture.

4. Simulation

In most applications, the dominant aberrations are low-order aberrations. The laser beam can get much improvement after low order Zernike aberrations corrected [19]. In this study, two different kinds of DMs (both have 19 elements and 10 mm effective aperture) were employed. The first DM (DM1) is a homemade unimorph deformable mirror with a high interactuator coupling [20]. The dual direction maximum defocus deformations of this DM are −14.3 μm and 14.9 μm. The 19 elements in the three inner rings were used for laser beam correction. The electrodes are arranged in the hexagon pattern, as shown in Fig. 1. The other DM (DM2) with low inter-actuator coupling is simulated according to piezoelectric stack DM [21] and BMC MEMS DM [22]. The influence function is in the form of Gaussian distribution and the interactuator coupling value

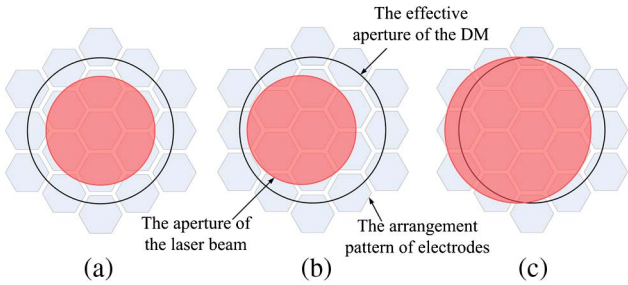

Fig. 1. Schematic illustration of (a) Case I: the aperture diameters do not match, (b) Case II: the two centers are not aligned, with the laser beam still in the DM effective aperture, and (c) Case III: the two centers are not aligned, with the laser beam exceeding the DM effective aperture.

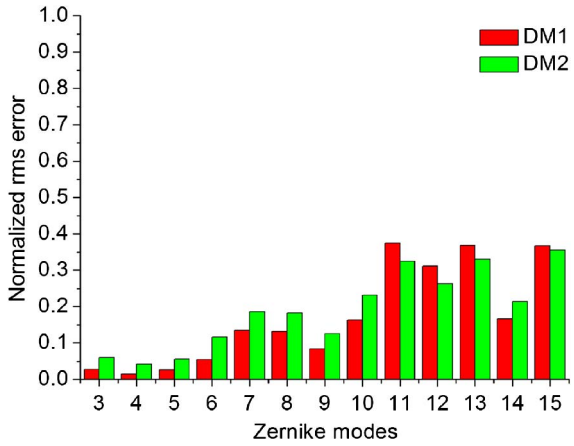

Fig. 2. Simulated normalized rms error for correction Zernike aberrations.

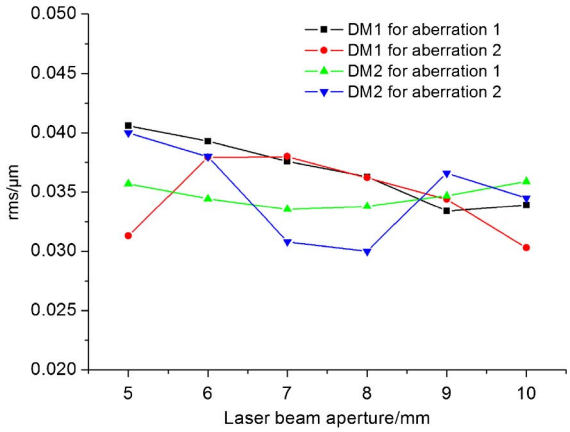

Fig. 4. Correction results for mismatched apertures: the DM's effective aperture was 10 mm and the laser beam aperture varied from 5 to 10 mm.

is 0.15. The simulated normalized root mean square (rms) errors for Zernike aberrations correction using these two DMs are shown in Fig. 2. It can be found that these two DMs have good correction ability for the 15th Zernike modes aberrations. Besides, the tip/tilt aberrations are usually corrected by tip/tilt mirror; thus only the third to the 15th Zernike modes are considered here.

In the simulation, two different aberrations were generated randomly to be the supposed aberration, denoted as aberration 1 and aberration 2. And the Zernike expansion coefficients of the two aberrations are shown in Fig. 3. The rms values of the two supposed aberrations were 150 and 385 nm, respectively. In correction process, the rms value of the residual wavefront aberration was selected to be the evaluation function. Both DM1 and DM2 are used to correct the supposed aberrations to analyze the effect of the mismatch problems.

For Case I, the effective aperture of DMs was 10 mm and the aperture diameter of the laser beam varied from 5 to 10 mm. The simulation results are shown in Fig. 4. When two different aberrations with different aperture change from 5 to 10 mm, the rms values of the residual wavefront after correction using DM1 and DM2 change less than 10 nm, as shown in Fig. 4. Compared to the initial rms values of the supposed aberrations, the rms values of the residual wavefront after correction have very little significant change. It can be found that similar correction results are achieved for different laser beam apertures mismatched with the DM effective aperture.

The simulation results of effects of center offset (Cases II, III) are shown in Fig. 5. For Case II, the laser beam aperture of 7 mm was selected, which was smaller than the DM's effective aperture (10 mm). To make sure the laser beam does not exceed the DM's effective aperture, the center offset is 0, 0.5, 1, and 1.5 mm, respectively. The residual wavefront rms errors after correction using DM1 increase from 36 to 40 nm for aberration 1 and increase from 38 to 45 nm for aberration 2 as the increase of center offset. The rms values after correction using DM2 for aberration 1 and aberration 2 also change less than 10 nm with the center offset changes [as shown in Fig. 5(a)]. It indicates that the offset of the center almost has little effect on the correction results. For Case III, the laser beam aperture was 10 mm; thus the laser beam would exceed the DM effective aperture with its center offset. As shown in Fig. 5(b), all the rms values of correction results for both two supposed aberrations and DMs increase rapidly with the increase of the offset. In other words, the correction results become worse with the increase of the center offset.

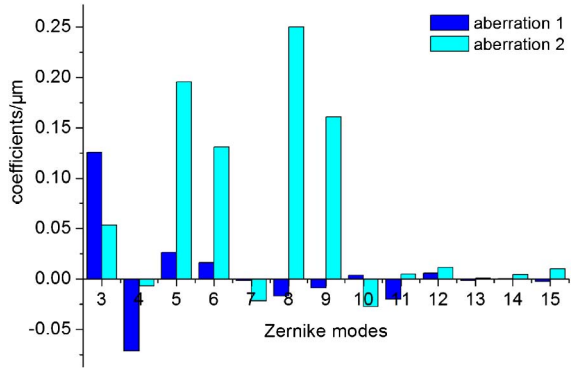

Fig. 3. Zernike coefficients of the generated wavefront.

5. Experiment Results

A. Experimental Setup

In order to evaluate the effect induced by the mismatches of the aperture diameter and the center position, an AO system for laser beam correction was established. The schematic of the experimental setup is illustrated in Fig. 6. A polarized 633 nm helium–neon laser was selected as the light source. After being expanded, the light beam passed through a beam splitter (BS) and reached the DM that was driven by 19-channel high-voltage amplifier (HVA). Here, the 19-element unimorph deformable mirror (DM1) was employed. Then the reflected beam from

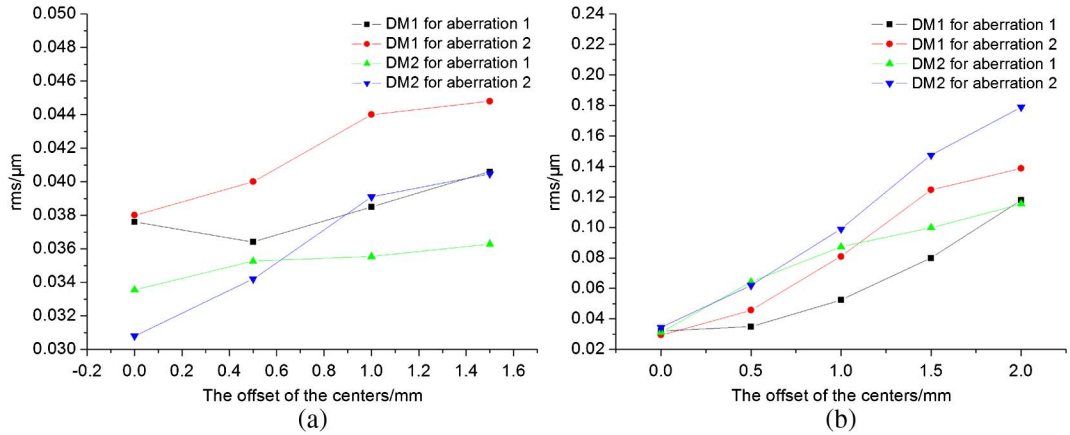

Fig. 5. Correction results for different center offsets. (a) The laser beam aperture did not exceed the DM's effective aperture. (b) The laser beam aperture exceeded the DM's effective aperture.

the DM passed through an aperture (AP). The size and center position of the laser beam to be corrected could be adjusted by the AP. Finally the laser beam was focused by a focus lens (FL, focus length 120 mm), and the focused spot was magnified 10 times by an objective lens (OL) and captured by a CCD camera.

B. Results and Discussion

In the experiments, the CCD-measured maximum intensity of the far field focal spot was selected as the evaluation function for the ZMHC algorithm, and the appropriate Zernike mode coefficients were found by the ZMHC algorithm in the closed-loop. The experiments for each situation were repeated 10 times to analyze the effect induced by the mismatches of the aperture diameter and center position.

To evaluate the effect of the mismatch of the aperture diameter (Case I), the aperture of the laser beam to be corrected was selected to change from 5 to 10 mm, and the effective aperture of the DM was constant (10 mm). The far field focal spots after correction with different apertures are shown in Fig. 7. It can be found that circular light spots have been achieved for all the apertures, though a few speckles appear around. It is known that the diameter of Airy disc's central spot can be calculated by equation: $D = 2.44\lambda f/d$. As the diameter of the laser beam changes from 5 to 10 mm, the size of the far field central spot also changes, which coincides with the calculated results based on the equation.

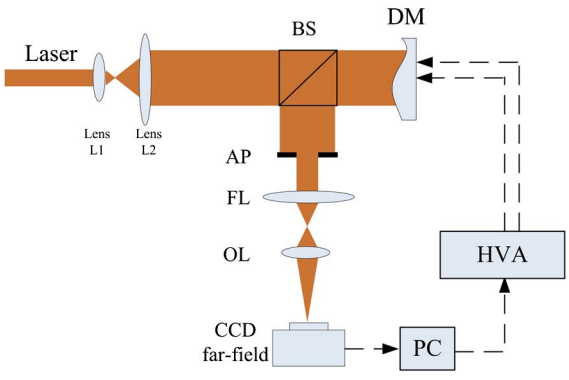

Fig. 6. Schematic illustration of the experimental setup for aberration correction.

Since the power of the laser could fluctuate during repeated tests, intensity concentration instead of the maximum light intensity was adopted to evaluate the corrected spots of different experiments, which is defined as the ratio of the intensity concentrated in the region of the Airy disc's central spot to the total sum of intensity in the whole region. The intensity concentration of all the results is calculated, and the average values and standard deviations of the concentration with different laser beam apertures are shown in Fig. 8. It is known that the ideal intensity concentrate of the Airy disc is about 83.8% [23]. As it is shown in Fig. 8, all the intensity concentration results have an average value about 0.75 with a small standard deviation less than 0.03. Comparing to the calculated intensity concentration with that of the Airy disc, it can be found that good correction results are achieved for all the laser beam apertures, which indicates the mismatch of the aperture has almost no effect on the laser beam correction results.

To analyze the effect from the mismatch of the center position, the experiments for Case II and Case III were performed, respectively. For Case II, the aperture of the laser beam was selected as 7 mm, which was smaller than the DM's effective aperture (10 mm). To make sure the laser beam does not exceed the DM's effective aperture, the center offset is from 0.5 to 1.5 mm. The far field focal spots after correction with different center offsets are shown in Fig. 9. From the correction results of different center offsets, it can be found that the central spots have the similar shape and maximum intensity. Besides, few speckles appear in all the spots in Fig. 9. So it can be seen that similar far field focal spots are achieved after correction. The average values and standard deviation values of the concentrations of different center offsets were calculated. The

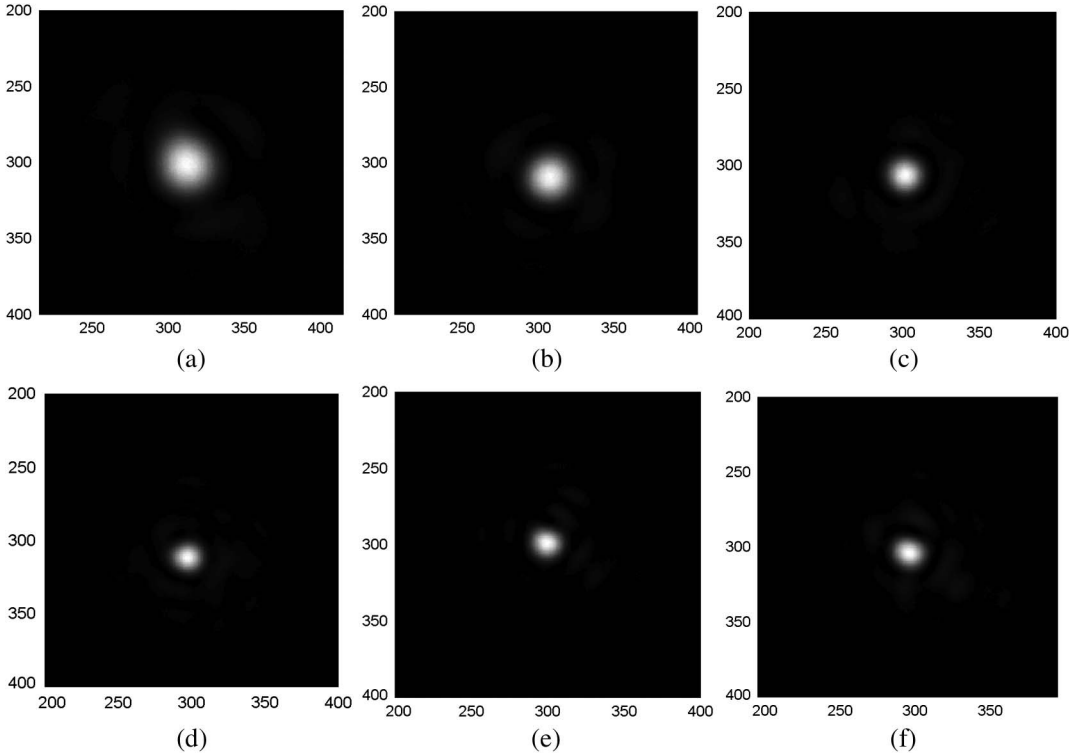

Fig. 7. Far field beam spots after correction with different apertures: (a) 5 mm, (b) 6 mm, (c) 7 mm, (d) 8 mm, (e) 9 mm, and (f) 10 mm.

results are shown in Fig. 10. It can be found that all the intensity concentrations results have an average value about 0.75 with a small standard deviation less than 0.02. The results of both the far field spots and the intensity concentration indicate that small offset between the centers of the laser beam and the DM's effective aperture will bring little effect on the correction results, when the laser beam does not exceeded the DM effective aperture.

For Case III, the aperture of the laser beam was selected as 10 mm, and the center offset between the laser beam and the DM effective aperture was set to be from 0.5 to 2 mm. As the increase of the offset value, the area of laser beam exceeding the DM's effective aperture increases. The far field beam spots after correction with different center offsets are shown in Fig. 11. It can be found that the central spot becomes worse in the respects of the shape and maximum intensity with the offset of the centers increasing. Besides, the amount of speckles also increases. The average values and standard deviation values of the concentration results are shown in Fig. 12. It can be found that the intensity concentrations become worse obviously even the center offset is only 0.5 mm. And the intensity concentrations become worse continuously with the center offset increasing. The results of both the far field spots and the intensity concentration indicate that the correction effect becomes worse rapidly as the offset of the two centers increases if the laser beam exceeds the effective aperture of the deformable mirror.

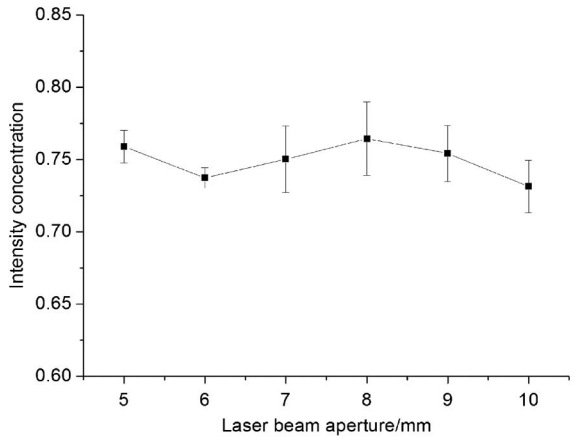

Fig. 8. Intensity concentration of the laser beam spots of different apertures.

From all the experimental results, it is demonstrated that the mismatches of the aperture diameter and the center position have almost no effect on the laser beam correction results, when the laser beam does not exceed the DM's effective aperture. And the same conclusion can be also drawn from the simulation results. The reason for that the mismatches have no effect on correction results in Case I and Case II can be considered simply as follows. Though the mismatches exist, the laser beam is still in the DM's effective aperture area. Here the DM controlled by the ZMHC algorithm can correct the wavefront aberrations in all the area of the effective aperture; thus the aberration of the laser beam area

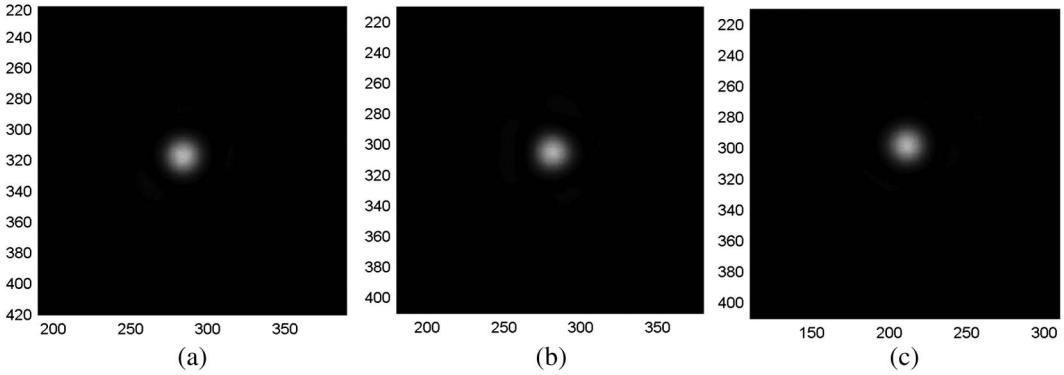

Fig. 9. Far field spots of 7 mm laser beam after correction with different offsets of the centers: (a) 0.5 mm, (b) 1 mm, and (c) 1.5 mm.

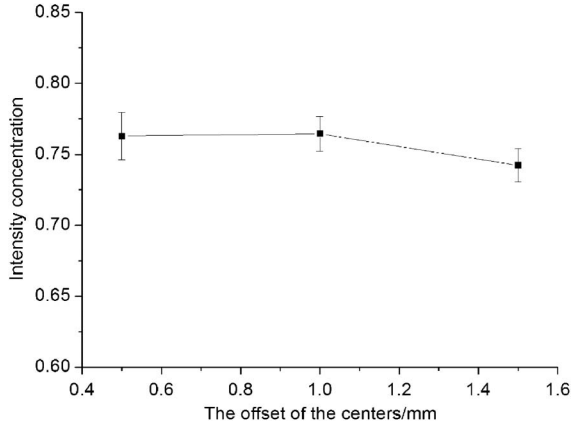

Fig. 10. Intensity concentration of the spots with different center offsets, when the laser beam did not exceed the DM effective aperture.

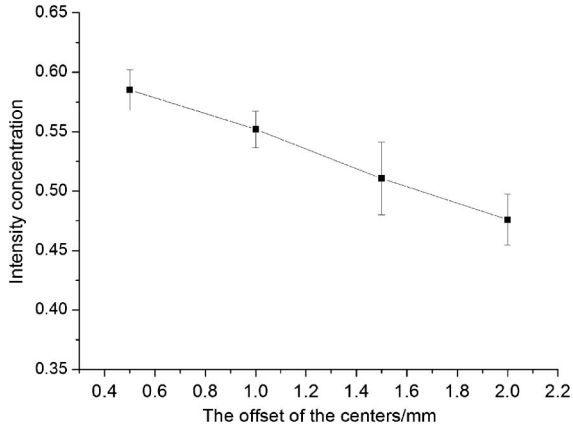

Fig. 12. Intensity concentration of the spots with different center offsets, when the laser beam exceeds the DM effective aperture.

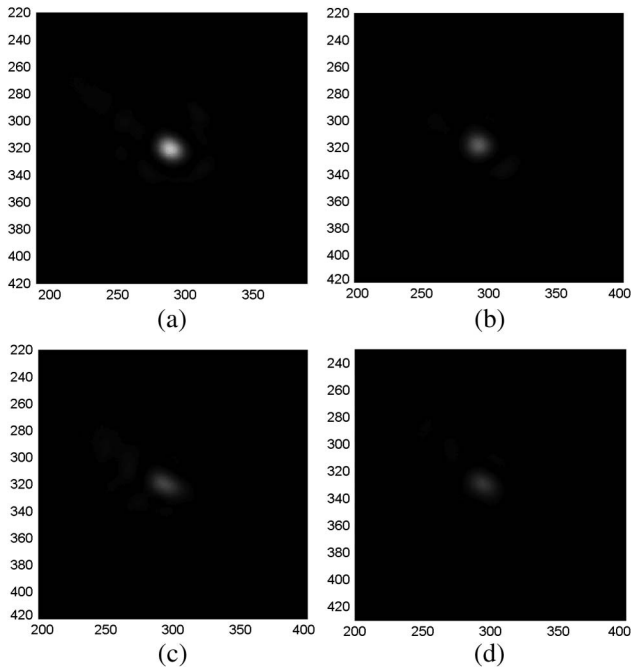

Fig. 11. Far field spots of 10 mm laser beam after correction with different offsets of the centers: (a) 0.5 mm, (b) 1 mm, (c) 1.5 mm, and (d) 2 mm.

is also corrected. However, when the laser exceeds the effective aperture with the offset of the centers, the correction ability out of the effective aperture become worse fast. It is the reason that the correction results become worse fast in the Case III.

6. Conclusion

This paper proposes a modified hill-climbing algorithm based on the Zernike modes for the laser beam correction and demonstrates its robustness. This algorithm adopts the Zernike mode coefficients instead of the actuators voltages as the adjustable variables. The effect on laser beam correction of the mismatches of the aperture size and the center position between the laser beam and the deformable mirror's effective aperture was investigated. The results of both simulations and experiments demonstrate that the mismatches of the aperture diameter and the center position have almost no effect on the laser beam correction results, unless the laser beam exceeds the DM's effective aperture. For this advantage, the alignment precision and aperture match demand of the laser beam correction system can be reduced, and this algorithm can have a wide application space in the wavefront sensor-less AO systems.

This work is supported by the National Basic Research Program of China (973 Program,

No. 2011CB302101), the National Natural Science Foundation of China (Grant No. 11303019) and China Postdoctoral Science Foundation (No. 2013M531521). The author also thanks the Material Science and Technology Center Development Foundation of Hefei (No. 2012FXCX002).

References

1. C. H. Rao, L. Zhu, X. J. Rao, C. L. Guan, D. H. Chen, S. Q. Chen, J. Lin, and Z. Z. Liu, "Performance of the 37-element solar adaptive optics for the 26 cm solar fine structure telescope at Yunnan Astronomical Observatory," Appl. Opt. **49**, G129–G135 (2010).
2. A. Guesalaga, B. Neichel, J. O'Neal, and D. Guzman, "Mitigation of vibrations in adaptive optics by minimization of closed-loop residuals," Opt. Express **21**, 10676–10796 (2013).
3. D. W. Arathorn, Q. Yang, C. R. Vogel, Y. H. Zhang, P. Tiruveedhula, and A. Roorda, "Retinally stabilized cone-targeted stimulus delivery," Opt. Express **15**, 13731–13744 (2007).
4. N. Doble and D. R. Williams, "The application of MEMS technology for adaptive optics in vision science," IEEE J. Sel. Top. Quantum Electron. **10**, 629–635 (2004).
5. O. Azucena, J. Crest, S. Kotadia, W. Sullivan, X. D. Tao, M. Reinig, D. Gavel, S. Olivier, and J. Kubby, "Adaptive optics wide-field microscopy using direct wavefront sensing," Opt. Lett. **36**, 825–827 (2011).
6. M. J. Booth, M. A. A. Neil, R. Juskaitis, and T. Wilson, "Adaptive aberration correction in a confocal microscope," Proc. Nat. Acad. Sci. USA **99**, 5788–5792 (2002).
7. T. A. Planchon, J. P. Rousseau, F. Burgy, and G. Cheriaux, "Adaptive wavefront correction on a 100 TW/10 Hz chirped pulse amplification laser and effect of residual wavefront on beam propagation," Opt. Commun. **252**, 222–228 (2005).
8. M. L. Gong, Y. T. Qiu, L. Huang, Q. Liu, P. Yan, and H. T. Zhang, "Beam quality improvement by joint compensation of amplitude and phase," Opt. Lett. **38**, 1101–1103 (2013).
9. P. Yang, W. Yang, Y. Liu, S. J. Hu, M. W. Ao, B. Xu, and W. H. Jiang, "19-element sensor-less adaptive optical system based on modified hill-climbing and genetic algorithms," Proc. SPIE **6723**, 31–37 (2007).
10. T. Planchon, W. Amir, J. J. Field, C. G. Durfee, and J. A. Squier, "Adaptive correction of a tightly focused, high-intensity laser beam by use of a third-harmonic signal generated at an interface," Opt. Lett. **31**, 2214–2216 (2006).
11. S. P. Poland, A. J. Wright, and J. M. Girkin, "Evaluation of fitness parameters used in an iterative approach to aberration correction in optical sectioning microscopy," Appl. Opt. **47**, 731–736 (2008).
12. H. T. Ma, Q. Zhou, X. J. Xu, S. J. Du, and Z. J. Liu, "Full-field unsymmetrical beam shaping for decreasing and homogenizing the thermal deformation of optical element in a beam control system," Opt. Express **19**, A1037–A1050 (2011).
13. P. Piatrou and M. Roggemann, "Beaconless stochastic parallel gradient descent laser beam control: numerical experiments," Appl. Opt. **46**, 6831–6842 (2007).
14. S. Zommer, E. N. Ribak, S. G. Lipson, and J. Adler, "Simulated annealing in ocular adaptive optics," Opt. Lett. **31**, 939–941 (2006).
15. R. El-Agmy, H. Bulte, A. H. Greenaway, and D. T. Reid, "Adaptive beam profile control using a simulated annealing algorithm," Opt. Express **13**, 6085–6091 (2005).
16. P. Yang, M. W. Ao, Y. Liu, B. Xu, and W. H. Jiang, "Intracavity transverse modes controlled by a genetic algorithm based on Zernike mode coefficients," Opt. Express **15**, 17051–17062 (2007).
17. Y. Liu, J. Q. Ma, B. Q. Li, and J. R. Chu, "Hill-climbing algorithm based on Zernike modes for wavefront sensorless adaptive optics," Opt. Eng. **52**, 016601 (2013).
18. M. J. Booth, "Wavefront sensorless adaptive optics for large aberrations," Opt. Lett. **32**, 5–7 (2007).
19. S. Chénais, F. Druon, F. Balembois, G. Lucas-Leclin, Y. Fichot, P. Georges, R. Gaumé, B. Viana, G. P. Aka, and D. Vivien, "Thermal lensing measurements in diode-pumped Yb-doped GdCOB, YCOB, YSO, YAG and KGW," Opt. Mater. **22**, 129–137 (2003).
20. J. Q. Ma, Y. Liu, T. He, B. Q. Li, and J. R. Chu, "Double drive modes unimorph deformable mirror for low-cost adaptive optics," Appl. Opt. **50**, 5647–5654 (2011).
21. P. Yang, Y. Ning, X. Lei, B. Xu, X. Li, L. Z. Dong, H. Yan, W. J. Liu, W. H. Jiang, L. Liu, C. Wang, X. B. Liang, and X. Tang, "Enhancement of the beam quality of nonuniform output slab laser amplifier with a 39-actuator rectangular piezoelectric deformable mirror," Opt. Express **18**, 7121–7130 (2010).
22. T. G. Bifano, P. Bierden, and S. A. Cornelissen, "MEMS deformable mirrors for space and defense applications," Proc. SPIE **6959**, 695914 (2008).
23. M. Born and E. Wolf, *Principles of Optics*, 6th ed. (Pergamon, 1983).